ACS OMEGA

http://pubs.acs.org/journal/acsodf

Article

Physicochemical Limitations of Capillary Models Applied to High-Concentration Polymer Solutions

David A. Schlachter, Martin D. Lennox, Basil D. Favis, Daniel Therriault, and Jason R. Tavares*

Cite This: *ACS Omega* 2022, 7, 5636−5645

Read Online

ACCESS | Metrics & More | Article Recommendations | Supporting Information

ABSTRACT: Advances in binder jet printing (BJP) require the development of new binder−powder systems, for example, to increase compatibility with better performance metal alloys or to increase the strength of parts using stronger binders. The dynamics of binder absorption are principally understood through capillary models. However, validation of these models in BJP has focused on variation of powder properties. Using a design-of-experiments approach and an optical observation method to track absorption of droplets, this study tests the influence of fluid properties on absorption time against the predictions of capillary models. Properties specific to polymeric binders, such as molecular weight and entanglement state, are also considered. Capillary models are found to be generally accurate in predicting absorption time in dilute systems; however, these predictions are not accurate for highly concentrated binder solutions. The effect of polymer entanglement becomes prevalent as the solution concentration increases, which can also potentially occur as a result of increased evaporation due to powder bed heating. Specifically, concentrated solutions close to the onset of entanglement will absorb much more slowly than predicted. Future models of BJP systems must account for the possibility of polymer entanglement throughout the absorption process. Improved models will provide a more accurate understanding of the flow and solidification of the binder in the powder, allowing faster development of new binders for improved performance in printing.

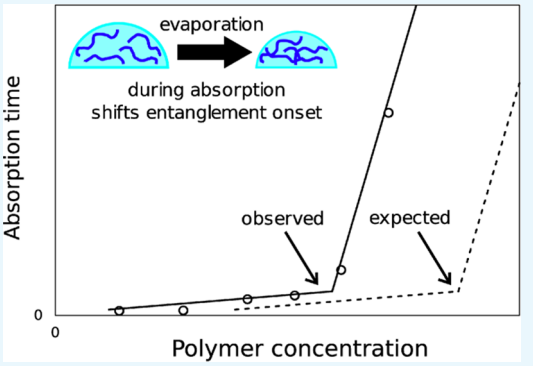

INTRODUCTION

Binder jet printing (BJP) is an additive manufacturing method well-suited to the fabrication of metal and ceramic parts.[1] In BJP, a binder is printed on the surface of a powder bed to bind together powder granules. Through printing on successive layers of fresh powder, a three-dimensional binder−powder composite is created, which must then be post-processed, often through thermal treatments that pyrolyze the binder and sinter the powder granules, significantly improving the mechanical properties of the part and reducing porosity. Further post-processing for improved mechanical properties, surface finish, and mechanical tolerances may be necessary.[2,3]

A significant limitation in developing a BJP process is the selection of printing parameters for a particular binder and powder. Many studies in this area have focused on the equilibrium saturation of the binder in a powder, with particular emphasis on the effect of granule size.[4−9] Studies in adjacent fields, such as wet granulation in pharmaceuticals or soil hydrology in civil engineering, have also contributed to understanding the equilibrium state of powder−binder composites.[10−13] Developments in the study of BJP contribute to this wider context of fluid infiltration of porous media. Additionally, advances in BJP support progress in many fields, such as tissue engineering, microelectronics, and pharmaceuticals.[14−16]

However, the dynamics of binder absorption play an important role in the printing process: the absorption time of a printed binder droplet limits the printing speed and the time between the spreading of new powder layers, and affects dimensional accuracy and droplet coalescence.[11,17,18] A better understanding of absorption dynamics in binder jetting would reduce development times by suggesting suitable printing parameters.

In considering the available models that predict the absorption dynamics of binders in BJP, theoretical models of binder−powder interaction have relied on capillary pressure to explain binder absorption into the powder bed.[4,5,19] In these models, the pores in the powder are modeled as bundles of parallel capillaries, where capillary forces drive absorption of the fluid.

These models have their basis in the Young−LaPlace equation,[20] expressed particularly by Washburn in his pioneering work on capillary dynamics,[21] which balances the Young−

Received: July 20, 2021
Accepted: January 27, 2022
Published: February 11, 2022

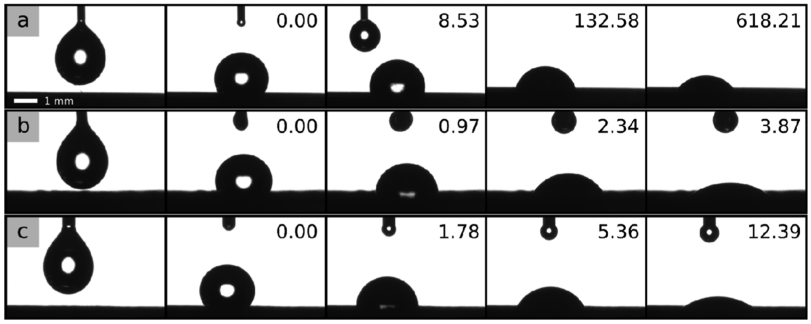

Figure 1. Representative droplet profiles: (left to right) before release, upon deposition, at 33 and 67% of target volume absorbed, and at endpoint (80% pre-impact volume absorbed), with time since deposition indicated, for (a) polyvinylpyrrolidone (PVP) 40k high μ high γ (Experiment 1,2), (b) PVA 10k low μ low γ (Experiment 2,5), and (c) PVP 40k low μ low γ (Experiment 1,5).

LaPlace equation with the Hagen−Poiselle equation to balance capillary and viscous forces as a fluid flows dynamically through a capillary. Marmur further developed a model for the absorption of small droplets into capillaries,[22,23] which was extended by Denesuk et al. for absorption into a powder.[24] Notably, Hapgood et al. tested the Denesuk model, modified it to better describe heterogeneous void spaces, and found it to reliably predict absorption time across several powders and fluids.[25] Recent models have built on these foundational studies with more detailed modeling of phenomena such as the changing radius of droplets on the surface and of infiltration within the powder bed.[26]

These models have been frequently applied to BJP. For example, Holman et al. proposed a model for binder absorption as a function of pore size, building on the Denesuk model.[27] Following similar principles, Moon et al. studied absorption kinetics in ceramic binder jetting, including an analysis of the relative effect of fluid properties, and proposed an equation based on Washburn capillary dynamics.[19] Extending the study of powder properties, Miyanaji et al. used Denesuk's model to estimate absorption time.[28] Bai et al. studied the effect on absorption when loading binders with nanoparticles, following the models of Hapgood and Denesuk.[29] The suitability of the models has recently been validated by Barui et al., who used X-ray synchrotron imaging to observe binder flow within the powder bed, comparing the dynamics to the Denesuk model.[30] The principal focus of these studies has been the effect of powder properties on absorption time, while consideration of the properties of the fluid has been limited. In the literature on binder jetting, these capillary models have been the principal approach for understanding binder absorption dynamics, particularly absorption time.

Setting aside the powder geometry, capillary models predict that a group of the properties of the fluid (γ: surface tension, μ: viscosity, θ: contact angle) will be proportional to the absorption time t

$$t \propto \frac{\mu}{\gamma \cos(\theta)} \tag{1}$$

The fluid property group in eq 1 represents a balance between capillary forces ($\gamma \cos\theta$), which drive absorption, and resistance from viscous forces (μ). Experimental validation of capillary models in BJP has often focused on the properties of the powder, rather than the effect of the fluid properties of the binder.[5,27,29]

In practice, the range of fluid properties suitable for BJP is limited by the dimensionless Ohnesorge number, which relates viscous forces (viscosity μ) to inertial and surface tension forces (density ρ, surface tension γ, droplet diameter L), as shown in eq 2.[31] Values ranging from 0.1 to 1 correspond to fluids that can be printed with ink jetting technologies.[32] Since BJP can utilize a range of drop sizes, the Ohnesorge number is an important consideration when designing and scaling systems.

$$\mathrm{Oh} = \frac{\mu}{\sqrt{\rho\gamma L}} \tag{2}$$

A class of binders of particular interest are aqueous solutions of organic polymers. These binders have shown promise as being easily solvable, producing environmentally friendly decomposition products, and being readily available for mass production.[33] Additionally, printing water-soluble polymers reduces environmental and safety concerns of other solvent-based systems. However, the applicability of capillary models to solutions of long-chain polymeric molecules in binder jetting has not been previously investigated. Studies of polymer adhesion to metals have shown a range of bonding mechanisms, depending on the charge of the metal surface and the chemistry of the binder.[34,35] Aqueous solutions of polymer interact with oxides on the metal surface, notably through hydroxyl groups on the polymer and metal.[36] In BJP, polymer−metal interfaces have been examined in the green body (after printing),[37] but studies of the interaction of bulk binder solution are also needed to improve printing performance. A better understanding of the impact of polymer properties on binder−powder interaction is important for the future development of polymeric binders.

The objective of this study is to investigate the extent to which the absorption dynamics of binders, particularly polymeric binders, can be predicted by the available capillary models. Since previous studies have focused on powder properties, the fluid properties of binders will be varied in this study according to a design-of-experiments (DOE) approach. In considering polymeric binders, capillary models do not directly account for their particular properties, such as molecular weight (see eq 1). The effect of polymer properties can be independently tested since solutions can be prepared at equivalent viscosity and surface tension from a variety of polymers, or of various molecular weights within the same polymer species. A model system using microliter scale droplets (larger than the picoliter droplets used in common binder jetting applications) will allow the influence of various parameters to be easily observed and linked to expected behaviors in production systems. By using an optical contact

https://doi.org/10.1021/acsomega.1c03857
ACS Omega 2022, 7, 5636−5645

angle method, the absorption times of binders can be efficiently measured, and the results are compared to the predictions of capillary models.

RESULTS AND DISCUSSION

Droplet Absorption. Representative droplet time profiles are presented in Figure 1. Across all runs, the average droplet volume in the video frame immediately before droplet release was 5.05 ± 0.71 μL.

Influence of Viscosity, Surface Tension, Molecular Weight, and Polymer Species. Experiment 1 (PVP binders only) studied the influence of viscosity, surface tension, and molecular weight, with mean effect plots shown in Figures 2 and S2. As predicted by capillary models, increased viscosity increases absorption times. On average, the effect of surface tension was not clear, with reduced effect at higher viscosity (see Figure S2). However, capillary models do not explain the significantly higher absorption times for high M_w binders (as compared to low M_w binders) at the same viscosity ($p = 2 \times 10^{-5}$). Since for each M_w of the polymer, different concentrations are required to reach the target viscosity, a relationship between polymer concentration and absorption time may exist.

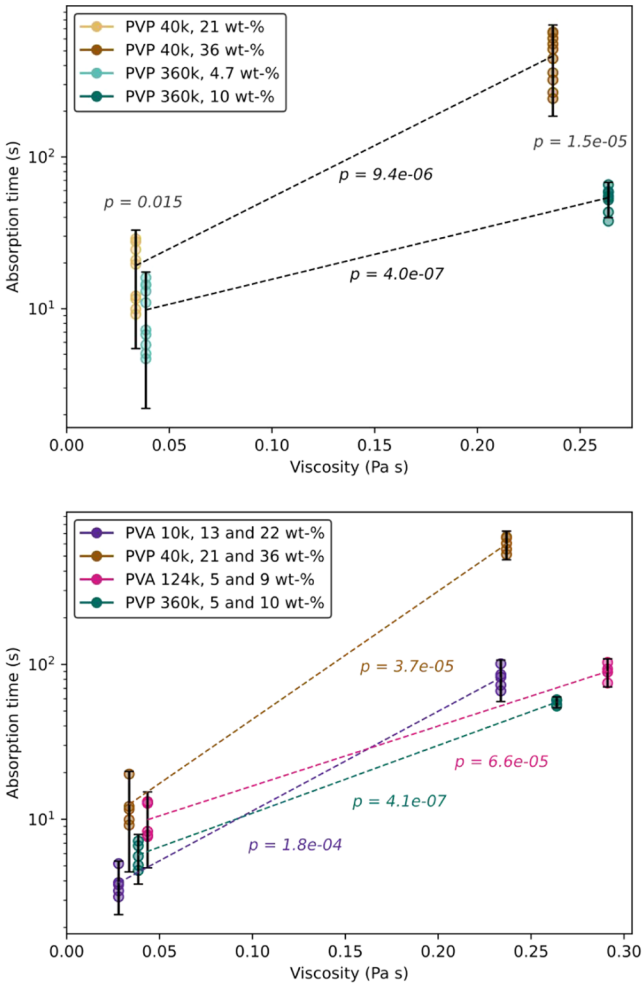

Figure 2. Mean effect plot showing effects of viscosity for aqueous PVP 40k and 360k binders (Experiment 1, top) and for PVP and PVA binders at constant surface tension (Experiment 2, bottom). Error bars: 95% CI (t-test), p-values: t-test.

In Experiment 2, the surface tension was held constant, and polymer species was included as a factor. Mean effect plots are shown in Figures 2 and S3. Again, viscosity has a strong effect on absorption time, which increases for all binders with increasing viscosity. However, at high viscosity, there are again significant differences between each polymer concentration. In particular, the most concentrated solution (PVP 40k 36 wt %) absorbs about 4 times more slowly than less-concentrated solutions at equivalent viscosity. For binders at similar viscosity and surface tension, the molecular weight was generally not significant (see Figure S3), except as will be discussed hereafter.

Capillary models predict similar absorption times for similar viscosity, surface tension, and contact angle (powder bed properties being equal). At low viscosity, droplet absorption times are similar in both PVA and PVP binder solutions (see Figure 2) regardless of molecular weight or concentration. Expected increases are observed for each binder with increasing viscosity, and moderate decreases are found with increased surface tension. However, because the available capillary models predict similar absorption times for similar fluid properties, an unexpected discrepancy is present at the high-viscosity levels, where more highly concentrated solutions have much longer absorption times.

In explaining this difference, concentration appears to play a dominant role. As seen in Figure 3, which shows the effect of concentration on absorption time, binders at similar viscosities would be expected to have similar resistance to capillary pressure and thus similar absorption times.

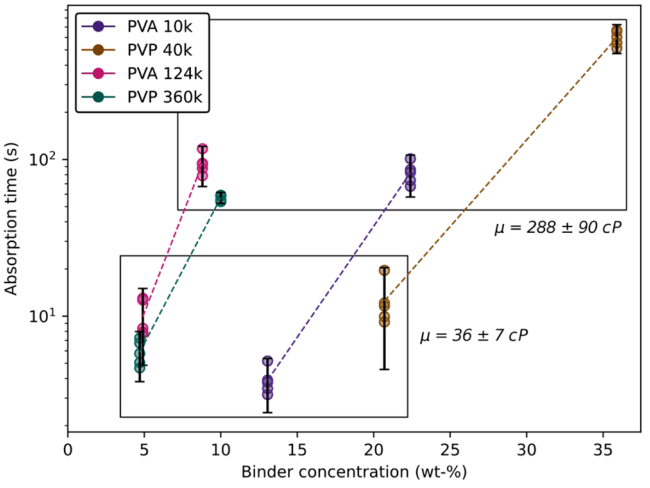

Figure 3. Effect of binder concentration on absorption time, for aqueous PVA and PVP binders at constant surface tension, with low- and high-viscosity samples indicated.

However, the PVP 40k binder at 35 wt % concentration has an average absorption time five times longer than the other binders that had been prepared at the same viscosity, but at a lower concentration of the binder. The second-order interaction plots (see Figures S4 and S5) confirm this relationship, showing a strong interaction effect on absorption time between molecular weight and viscosity. This interaction is again linked to concentration since a higher concentration of a lower-molecular-weight polymer is required to reach the same viscosity as a solution prepared using a high-molecular-weight polymer.

https://doi.org/10.1021/acsomega.1c03857
ACS Omega 2022, 7, 5636−5645

Absorption Time by the Capillary Property Group. Using the contact angles determined by the Washburn capillary method (see Table S2), the absorption time was compared to the capillary property group, as shown in Figure 4. Within each combination of binder and molecular weight, absorption times follow the property group with expected linear trends.

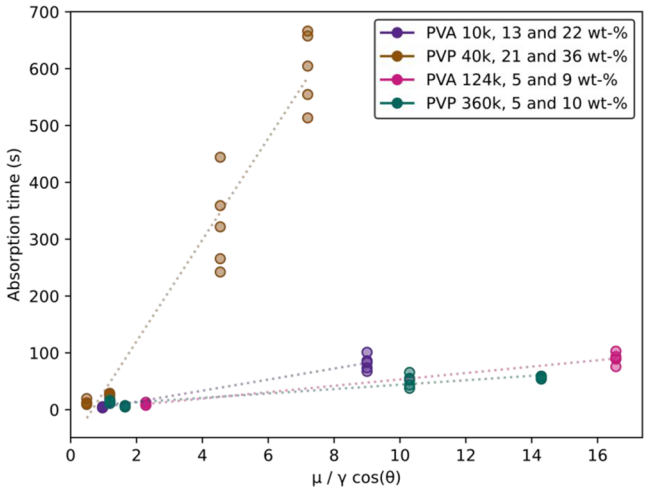

Figure 4. Absorption time versus capillary property group ($\mu/\gamma \cos\theta$) for aqueous PVP and PVA, with linear regressions shown for each molecular weight of each binder.

Plotted against the capillary property group, the absorption times of the highly concentrated PVP seem to follow a different regime than the other binders (Figure 4). Since the surface tension, viscosity, and contact angle are similar between this binder and other high-viscosity binders, it would be expected that absorption times would be similar. The trend of absorption time against the capillary property group is generally consistent for the less-concentrated binder solutions but does not explain the behavior at high concentrations. Interestingly, the relationship between absorption time and the capillary property group appears to hold very well within each binder, with a spread in the data for each binder attributable to any irregularities in powder packing.[25] It should be noted that the relative error in average absorption time for each binder is similar between replicates (±20% of each average measure), despite larger absolute errors for long absorption times. If the true average within each set of data points is supposed as being either the maximum or minimum value, the significant difference between observed and expected trends still holds.

A possible explanation for the behavior of concentrated binder solutions is that the solutions approach critical entanglement concentrations, where chain−chain interactions would be expected to significantly slow absorption into the powder bed. However, plots of log(viscosity) for each solution do not clearly manifest the inflection point indicative of the onset of entanglement (see Figure S1) and so cannot verify that the solutions are in a concentrated regime where entanglement dominates.[38]

However, theoretical calculation of entanglement concentration is possible for each binder. The entanglement molecular weight of a polymer in solution at a given concentration, $(M_c)_{soln}$, is approximately equal to the quotient of the entanglement concentration in the melt M_c (values readily available[39,40] in the literature) and the volume fraction φ,[41] as shown in eq 3

$$(M_c)_{soln} = \frac{M_c}{\phi} \tag{3}$$

As shown in eq 4, the solution entanglement number $(\eta_e)_{soln}$ (average number of entanglements) is the ratio of the molecular weight of the polymer M_w and the entanglement concentration in solution $(M_c)_{soln}$

$$(n_e)_{soln} = \frac{M_w}{(M_c)_{soln}} = \frac{\phi M_w}{M_c} \tag{4}$$

The onset of entanglement in solution occurs when $(\eta_e)_{soln}$ is approximately equal to two since each entanglement requires two chains. However, electrospinning studies suggest that the onset of entanglement is a gradual process that occurs between values of $(\eta_e)_{soln}$ from 2 to 3.5, depending on the polymer system.[42] For the solutions used in this study, estimated entanglement concentrations are shown in Figure 5.

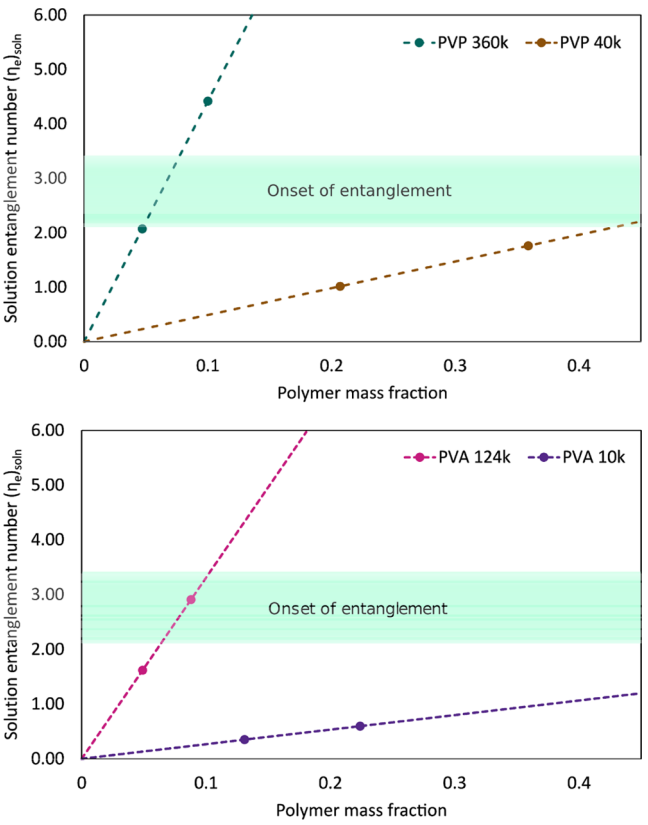

Figure 5. Calculated dependence of the solution entanglement number on polymer concentration for PVA and PVP solutions. Concentrations used in this study indicated by points, green shaded regions indicate the approximate onset of entanglement, and dotted lines show the theoretical function of the entanglement number on concentration.

To study the effect of entanglement on absorption dynamics, the absorption times of the binders were plotted against the solution entanglement number (see Figure S6). While more entangled solutions of the same polymer had consistently higher absorption time, a general trend is not apparent. In particular, concentrated PVP 40k absorbs more slowly than other binders at a similar level of entanglement. On the other

https://doi.org/10.1021/acsomega.1c03857
ACS Omega 2022, 7, 5636−5645

hand, solutions with similar viscosity (see Figure 3) have similar absorption times over a wide range of the solution entanglement number.

The level of entanglement of the binder solution as-prepared at room temperature has a weak effect on absorption time, compared to other properties such as viscosity, concentration, or the capillary property group.

Influence of Temperature. In the BJP process, powder beds are typically heated to accelerate the evaporation of solvent and solidification of the part. The effect of heating on absorption time is shown in Figure 6. In all cases, heating increased absorption times.

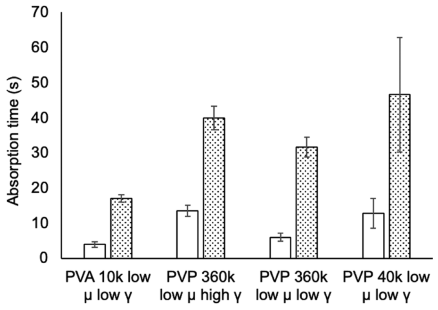

Figure 6. Absorption time of binders at room temperature (white) and 60 °C (gray).

In heated powder beds, capillary models predict that absorption time will decrease for aqueous binders since decreased viscosity would have a stronger effect than moderate decreases in surface tension. However, the opposite trend is observed experimentally. It is likely that evaporation of solvent rapidly increases the concentration of the binder in heated droplets, correspondingly increasing the viscosity. To explore this hypothesis, the evaporation rates of 5 μL water droplets on stainless steel plates at 60 °C were observed. For a droplet of binder under similar conditions, the estimated viscosity and polymer concentration were calculated as a function of time (Figure 7). A rapid increase in viscosity is predicted, supporting the idea that at high concentrations of the binder, even small amounts of evaporation can significantly increase absorption time. At the picoliter scale, typical of BJP, this effect can be potentially be mitigated, as the time scale for absorption

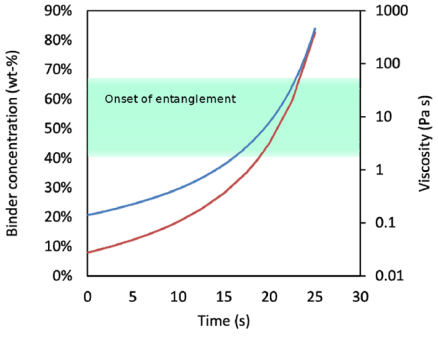

Figure 7. Calculated binder concentration (blue) and viscosity (orange) of a 5 μL droplet of the 20% PVP 40k binder undergoing evaporation on a 60 °C stainless steel plate, based on the evaporation rate of water under these conditions (see Figure S8) and viscosity standard curves.

into the powder is typically much shorter than that for evaporation.[18,43]

Similar behavior to the unexpectedly slow absorption of concentrated polymer solutions shown in this study has been observed for PVP in electrospinning, where it is hypothesized that high concentrations of low M_w polymer solutions rapidly form skins on exposure to air.[44,45] Such a phenomenon would significantly increase resistance to capillary forces, slowing absorption. This effect would be amplified by heating the powder bed.

When considering the effect of entanglement on the theoretical absorption profile shown in Figure 7, it is clear that an entangled state could be quickly achieved even if the initial solution is comparatively dilute. For the modeled 20 wt % PVP 40k binder, however, absorption in all experiments was complete before the predicted onset of an entangled state, calculated to occur at roughly 15 or 20 s.

When considering a PVP droplet at the higher concentration tested (35 wt %) under the conditions tested in these experiments, the entangled regime would quickly be reached by evaporation. At sufficiently high local concentrations, gel formation would occur, forming a skin, as previously mentioned. Thus, at high concentrations of polymers, small amounts of evaporation will lead to highly viscous states that will absorb more slowly than the initial fluid properties would predict. While the timescales shown in this Figure are surely shorter than would occur in a powder bed, the effect of rising viscosity with evaporation could affect a sufficiently heated process. To test this hypothesis, additional solutions of PVP 40k were prepared at various concentrations, following the methodology previously described to measure the absorption time of droplets. As can be seen in Figure 8, small increases in

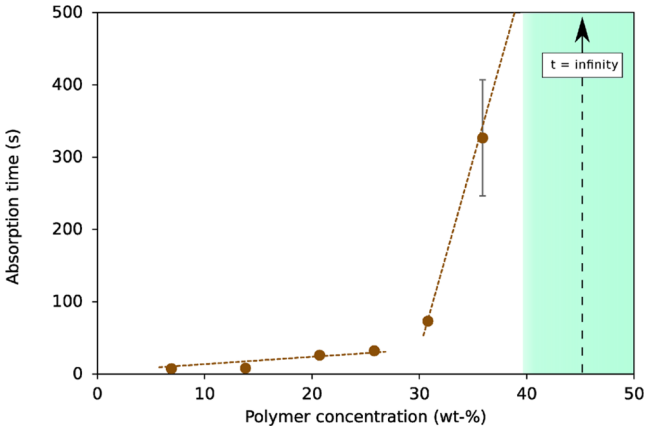

Figure 8. Experimental absorption times for PVP 40k solutions at various as-prepared concentrations. Note infinite absorption time at 45 wt % (droplet solidifies on bed surface). Green shaded region: predicted entangled regime. Dotted linear fit lines are added to guide the eye.

the as-prepared concentration led to dramatic increases in absorption time, with a 45% solution having infinite absorption time (droplet solidifies on powder surface). This result shows that highly concentrated binders will absorb more slowly than expected so long as small amounts of evaporation are able to rapidly change their properties. The intersection of the lines in Figure 8 gives the inflection point where the as-prepared solution concentration begins to give rise to polymer entanglement phenomena. It should be noted that, due to

https://doi.org/10.1021/acsomega.1c03857
ACS Omega 2022, 7, 5636−5645

solvent evaporation in the heated bed, the actual solution concentration is higher at the moment the absorption time measurement is recorded. In other words, although the as-prepared solution is a key controlling parameter, the actual true solution concentration for entanglement is at a higher value. Obtaining that value would require estimating the evaporation effect due to the heated bed and is beyond the scope of this paper. However, some important suggestions will be given below on solution preparation and how to avoid polymer entanglement phenomena in the heated bed.

Models of binder jetting have not, to this point, considered polymer entanglement as affecting the absorption time of droplets. The two regimes suggested in the plot of absorption time vs concentration (Figure 8) invoke the traditionally understood relationship between viscosity and concentration, which may be expected since absorption time has been predicted to be proportional to the viscosity. However, the calculations of solution entanglement number versus concentration for the initial solution, compared to concentration at which the inflection point is observed in the absorption time vs concentration chart, point to the change in viscosity throughout the absorption process. These observations demonstrate that the assumption that viscosity is constant when modeling the printing of droplets in binder jetting must be validated.

While heating can slow absorption timescales, insufficient or uneven heating reduces printing accuracy because it does not allow for absorption of excess binders from newly printed layers, as recently shown by Crane.[46] To improve flowability of a binder, our results show that it is preferable to use higher-molecular-weight polymers at lower concentrations to reach fluid property targets such as viscosity. The effect of evaporation on binder absorption can be estimated by considering the evaporation rate of solvent and the corresponding estimated increase in viscosity of the binder as it is absorbed. High concentrations of polymer that are close to entanglement concentrations should be avoided since very small amounts of evaporation will significantly affect binder properties.

When the powder bed is heated between layer deposition, solvent is evaporated and binder concentration may increase significantly. In these conditions, polymeric binders will reach very high viscosities within the powder bed. As entanglement concentrations are reached, binder mobility will be reduced. Since binder interaction between layers is important in creating parts with favorable mechanical properties, binder solutions must be prepared such that entanglement concentrations will not be reached prematurely in the heated powder bed. Interactions between layers are key to adhesion and the formation of polymer bridges between particles,[37] and sufficient binder mobility must be maintained between layer deposition to ensure adequate layer adhesion.

It must be emphasized that the microlitre-scale droplets used in this study differ in many important respects from picolitre-scale printing systems commonly used in binder jetting today. For example, the absorption time of a single droplet in today's binder jetting systems is usually complete within a few milliseconds, whereas evaporation of such a droplet may occur on the order of several seconds.[43] However, further development and broader applications of binder jetting systems can be expected to push beyond these operating limits. Such systems could include those with high concentrations of the binder solute or with highly volatile solvents (particularly at high temperatures). Indeed, increasing polymer concentration is a natural approach to decrease binder volumes. Due to the limitations of commercial printing systems, these types of binder jetting environments are not in common use. The findings of this study, namely, that polymer entanglement can have an important effect on a printing process involving the absorption of polymerics solutions into powder beds, will be an important guide to those developing innovative powder-based printing systems.

Unexpected printing behavior, particularly very slow absorption times, can be avoided by performing the experiment suggested by Figure 8 for a particular combination of the binder, solvent, and substrate, ideally at the target bed temperature. The inflection point in the plot of absorption time versus solution concentration (as-prepared) will indicate the practical concentration at which entanglement becomes significant, considering the actual evaporation of the solvent. Binder solutions below the practical entanglement concentration will behave more predictably than solutions above. For example, as shown in Figure 8, entanglement is predicted at 40% but is observed at 30%. In this particular system, polymer concentrations in the as-prepared solutions should not exceed 30% for efficient absorption times. Where the slope of the curve after entanglement is quite large, the behavior will be unpredictable and absorption times will be much longer than capillary models would predict.

Further work will be needed to clearly establish threshold concentrations above which capillary models provide unreliable predictions. Future models of droplet absorption in binder jetting must take into account the effects of heating and evaporation, enabling more industrially relevant predictions to advance the development of new binders.

CONCLUSIONS

Understanding printing dynamics in BJP will be essential to the development of new printing systems. The available capillary models may be adequate for predicting the absorption time of fluids with similar compositions at low concentrations, such as those used in many current binder jetting systems. However, it has been shown in this paper that properties such as molecular weight and concentration play an important role in absorption dynamics in binder jetting. Specifically, binder solutions at high concentrations close to entanglement concentrations have significantly increased absorption times when compared to less-concentrated solutions at the same viscosity (for example, solutions of a higher-molecular-weight polymer). One mechanism that can exacerbate the entanglement effect is evaporation. While existing models may be adequate for many current binder jetting systems, future designs with highly concentrated solutions or volatile solvents must account for polymer entanglement, which can play a significant role in the dynamics of printing systems. The design of new binder systems for BJP requires trade-offs between flowability and setting time that may be further described by subsequent investigation of these phenomena. The existing capillary models of binder jet printing must be expanded to account for these factors, allowing more rapid development of new binder systems for increased part strength and printing performance.

https://doi.org/10.1021/acsomega.1c03857
ACS Omega 2022, 7, 5636−5645

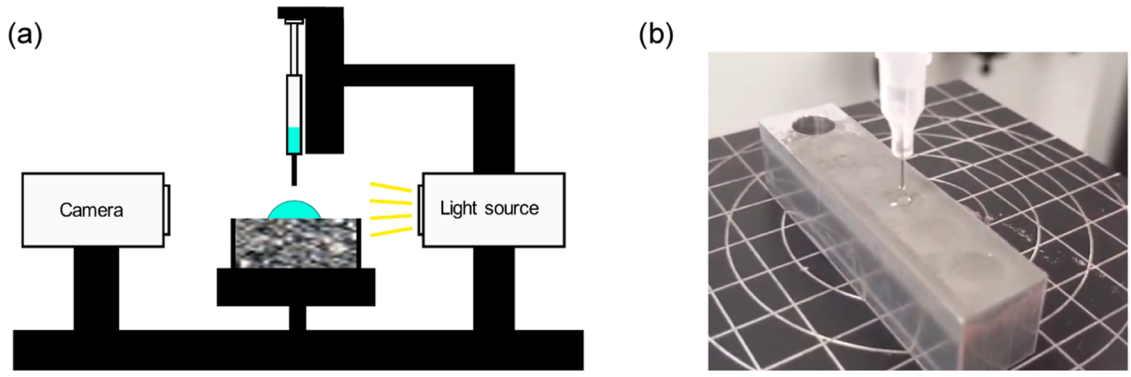

Figure 9. Schematic of apparatus for droplet absorption (a) and photo of well plate and powder surface (b) during the experiment.

Table 1. Design for Experiments 1 (PVP Binders) and 2 (PVA & PVP Binders)

experiment no.	run no.	binder	surface tension (mN m^{-1})	molecular weight	viscosity (mPa s)	Ohnesorge no.
1	1	PVP	45	40 000	270	1
	2	PVP	65	40 000	270	1
	3	PVP	45	360 000	270	1
	4	PVP	65	360 000	270	1
	5	PVP	45	40 000	27	0.1
	6	PVP	65	40 000	27	0.1
	7	PVP	45	360 000	27	0.1
	8	PVP	65	360 000	27	0.1
2	1	PVA	45	10 000	270	1
	2	PVP	45	40 000	270	1
	3	PVA	45	124 000	270	1
	4	PVP	45	360 000	270	1
	5	PVA	45	10 000	27	0.1
	6	PVP	45	40 000	27	0.1
	7	PVA	45	124 000	27	0.1
	8	PVP	45	360 000	27	0.1

MATERIALS AND METHODS

Materials. PVA and PVP have been frequently reported in the polymeric BJP literature and are readily available and well-characterized polymers;[33,47−50] thus, they will serve as test molecules in the present study. Poly(vinyl alcohol) (PVA) (Sigma-Aldrich: M_w = 9000−10 000, 80% hydrolyzed; M_w = 85 000−124 000, 87−89% hydrolyzed) and polyvinylpyrrolidone (PVP) (Alfa Aesar: M_w = 40 000; M_w = 360 000) were used to create aqueous binders by dilution with deionized water. Surface tension adjustment was performed with Pluronic F68 surfactant (10% aqueous solution) (Gibco). Stainless steel 316L spherical powder (D_{10} = 7 μm; D_{50} = 12 μm; D_{90} = 19 μm, see size distribution in Figure S7) was used as the substrate for absorption experiments. As a baseline for capillary rise measurements, hexanes (n- and cyclo-, Fisher) were used.

Binder Preparation. To prepare binders according to the experimental design, standard curves for viscosity versus polymer concentration were used to prepare solutions at high- and low-viscosity levels (270 and 27 mPa s) for each combination of polymer species and molecular weight, by dilution of the polymer in deionized water (see Figure S1). Pluronic F68 was added in concentrations from 0.001 to 0.1%, as required to reach the 45 mN/m target. Viscosities were measured using an Anton Paar MCR-501 rheometer (geometry DG26.7, Pelletier module C-PTD200) at 25 °C, with decreasing shear rates from 1000 to 0.1 s^{-1}. Surface tensions were measured by the pendant drop method (OCA20, DataPhysics Instruments). Measured values of binder properties are shown in Table S1.

Droplet Absorption. Droplet absorption experiments were performed using an optical contact angle measuring system (OCA20, DataPhysics Instruments), consisting of a video camera observing deposition of a backlit liquid droplet by a syringe (see Figure 9). The target volume to deliver was 5 μL, controlled by using tip sizes ranging from 0.24 to 0.52 mm outer diameter (Optimum Dispense Tips, Nordson EFD), according to the properties of each fluid. Droplets were released from 0.5 mm above the powder bed. Video analysis software (SCA20, DataPhysics Instruments) was used to determine the drop volume before release and to track the binder volume remaining on the surface throughout the absorption process.

Powder beds of 316L stainless steel were prepared in fabricated aluminum well plates, designed to separate replicates and have a smooth, level surface to facilitate imaging. The powder was poured into each well, gently tapped, and leveled, thus simulating powder deposition in a binder jetting production process.[8,29] Trials to compare wells prepared using this method against compacted beds (tapped and compressed with a glass rod) resulted in a variation in absorption times on the order of ±10% between methods, an error similar to the variability between replicates under either preparation method.

After depositing each droplet, the volume of liquid above the powder surface was tracked with respect to time, and

https://doi.org/10.1021/acsomega.1c03857
ACS Omega 2022, 7, 5636−5645

absorption time was calculated as the time between deposition of the droplet on the powder bed and the time at which 80% of the dispensed volume had been absorbed.[29] Measuring absorption time on a volume basis, rather than by simply tracking the contact angle, is preferable since this approach is independent of the dynamics of the change in radius and of the receding contact angle characteristic of each fluid−powder system. Five replicates were performed for each run, with absorption times averaged.

Washburn Capillary Rise. The Washburn capillary rise method was used to calculate binder−powder contact angles.[51] Following the previously described methodology,[53,52] borosilicate glass capillaries (inner diameter: 8 mm) were plugged with 0.2 g cotton and then filled with 6 g stainless steel powder. Each tube was tapped at least 100 times to a uniform level to control powder packing. Tubes were suspended from an analytical balance, and a beaker of the binder was raised so that the surface of the liquid binder was level with the bottom of the tube. Experiments were performed for each of the binders, as well as for a totally wetting liquid (hexanes, contact angle = 0°) as the reference. The squared rate of mass increase was plotted and used to determine the contact angles, as shown in Table S2.

Temperature Control. To study the influence of temperature on binder absorption time, an electric Peltier heating unit (TEC 160, DataPhysics Instruments) was used to maintain the surface temperature of the powder bed at a level within the range of industrial interest (60 °C). Temperatures were verified using thermocouples (DataPhysics) as well as an infrared thermometer (Extech 42510A).

Experimental Design. To study the influence of binder properties on absorption time, two full factorial experimental designs, summarized in Table 1, were elaborated, varying: (1) surface tension, molecular weight, and viscosity for PVP binders and (2) molecular weight, viscosity, and polymer species for both PVA and PVP binders. While a single experiment (full factorial, four factors) had been originally designed, the low surface tension of PVA solutions precluded high−low surface tension levels for this binder. For Experiment 1, the range of surface tensions was selected with high values unadjusted (65 mN/m) and low values adjusted using a surfactant. In Experiment 2, the surface tension of the PVP binders was adjusted to match the (lower) surface tension of the PVA binders. Molecular weights were selected to give similar viscosities at equivalent concentrations between species.

Viscosities were selected such that the Ohnesorge numbers of the fluids would correspond to the maximum and minimum jettable viscosities within the test system, to test the range of relevant properties with consideration of the scale of the system.

■ ASSOCIATED CONTENT

Supporting Information

The Supporting Information is available free of charge at https://pubs.acs.org/doi/10.1021/acsomega.1c03857.

Measured properties of binder solutions and powder; additional mean effects and interaction plots (PDF)

■ AUTHOR INFORMATION

Corresponding Author

Jason R. Tavares − *Department of Chemical Engineering, CREPEC (Research Center for High Performance Polymer and Composite Systems), Polytechnique Montreal, Montreal, Quebec H3T 1J4, Canada;* orcid.org/0000-0002-3828-2993; Email: jason.tavares@polymtl.ca

Authors

David A. Schlachter − *Department of Chemical Engineering, CREPEC (Research Center for High Performance Polymer and Composite Systems), Polytechnique Montreal, Montreal, Quebec H3T 1J4, Canada*

Martin D. Lennox − *Department of Chemical Engineering, CREPEC (Research Center for High Performance Polymer and Composite Systems), Polytechnique Montreal, Montreal, Quebec H3T 1J4, Canada*

Basil D. Favis − *Department of Chemical Engineering, CREPEC (Research Center for High Performance Polymer and Composite Systems), Polytechnique Montreal, Montreal, Quebec H3T 1J4, Canada;* orcid.org/0000-0002-7980-3740

Daniel Therriault − *Laboratory for Multiscale Mechanics, Department of Mechanical Engineering, CREPEC (Centre for Applied Research on Polymers and Composites), Montreal, Quebec H3T 1J4, Canada;* orcid.org/0000-0002-4456-9472

Complete contact information is available at: https://pubs.acs.org/10.1021/acsomega.1c03857

Notes

The authors declare no competing financial interest.

■ ACKNOWLEDGMENTS

The authors acknowledge financial support from NSERC (Natural Sciences and Engineering Research Council of Canada) (grant number CRDPJ 532147), Prima-Québec (grant number R16−13−002), Les Industries Sautech, Kinova Robotics, and CREPEC (Centre for Applied Research on Polymers and Composites). The principal author (D. Schlachter) further acknowledges scholarship support from FRQNT (Fonds de recherche du Québec − Nature et technologies) (scholarship number 272300) and Rio Tinto.

■ ABBREVIATIONS

BJP, Binder jet printing; PVA, Poly(vinyl alcohol); PVP, Polyvinylpyrrolidone; M_w, molecular weight

■ REFERENCES

(1) Ziaee, M.; Crane, N. B. Binder Jetting: A Review of Process, Materials, and Methods. *Addit. Manuf.* **2019**, *28*, 781−801.

(2) Cima, M.; Sachs, E.; Fan, T.; Bredt, J. F.; Michaels, S. P.; Khanuja, S.; Lauder, A.; Lee, S.-J. J.; Brancazio, D.; Curodeau, A. et al. Three-Dimensional Printing Techniques. US5387380A1995.

(3) Sachs, E. M.; Haggerty, J. S.; Cima, M. J.; Williams, P. A. Three-Dimensional Printing Techniques. US5204055A1993.

(4) Bredt, J. F. Binder Stability and Powder/Binder Interaction in Three Dimensional Printing. PhD Thesis, Massachusetts Institute of Technology, 1995.

(5) Miyanaji, H.; Zhang, S.; Yang, L. A New Physics-Based Model for Equilibrium Saturation Determination in Binder Jetting Additive Manufacturing Process. *Int. J. Mach. Tools Manuf.* **2018**, *124*, 1−11.

(6) Miyanaji, H.; Yang, L. Equilibrium Saturation in Binder Jetting 3D Printing Process: Theoretical Model vs. Experimental Observations. In *Proceedings of the 27th Annual International Solid Freeform Fabrication Symposium, Austin, TX, August 8 − 10, 2016;*, Austin, TX, August 8−10, 2016; Seepersad, C.; Bourell, D.; Marcus, H.; Beaman,

J.; Crawford, R.; Fish, S., Eds.; University of Texas at Austin, 2016; pp 7−10.
(7) Colton, T.; Liechty, J.; McLean, A.; Crane, N. Influence of Drop Velocity and Droplet Spacing on the Equilibrium Saturation Level in Binder Jetting. In *Solid Freeform Fabrication 2019: Proceedings of the 30th Annual International Solid Freeform Fabrication Symposium − An Additive Manufacturing Conference, Austin, TX, August 12 − 14, 2019.*; Austin, TX, August 12−14, 2019. Seepersad, C.; Bourell, D.; Kovar, D.; Beaman, J.; Crawford, R.; Fish, S., Eds.; University of Texas at Austin, 2019; pp 99−108.
(8) Chun, S.-Y.; Kim, T.; Ye, B.; Jeong, B.; Lee, M.; Lee, D. H.; Kim, E.-S.; Lee, H.; Kim, H.-D. Capillary Pressure and Saturation of Pore-Controlled Granules for Powder Bed Binder Jetting. *Appl. Surf. Sci.* **2020**, *515*, No. 145979.
(9) Colton, T.; Crane, N. B. Influence of Droplet Velocity, Spacing, and Inter-Arrival Time on Line Formation and Saturation in Binder Jet Additive Manufacturing. *Addit. Manuf.* **2021**, *37*, No. 101711.
(10) Emady, H. N.; Kayrak-Talay, D.; Schwerin, W. C.; Litster, J. D. Granule Formation Mechanisms and Morphology from Single Drop Impact on Powder Beds. *Powder Technol.* **2011**, *212*, 69−79.
(11) Mundozah, A. L.; Cartwright, J. J.; Tridon, C. C.; Hounslow, M. J.; Salman, A. D. Hydrophobic/Hydrophilic Static Powder Beds: Competing Horizontal Spreading and Vertical Imbibition Mechanisms of a Single Droplet. *Powder Technol.* **2018**, *330*, 275−283.
(12) Lee, A. C. S. Formulation of Granule Nuclei under Static and Dynamic Powder Bed Conditions. PhD Thesis, Purdue University, 2011.
(13) Sposito, G. The "Physics" of Soil Water Physics. *Water Resour. Res.* **1986**, *22*, 83S−88S.
(14) Poomathi, N.; Singh, S.; Prakash, C.; Subramanian, A.; Sahay, R.; Cinappan, A.; Ramakrishna, S. 3D Printing in Tissue Engineering: A State of the Art Review of Technologies and Biomaterials. *Rapid Prototyping J.* **2020**, *26*, 1313−1334.
(15) Zhang, W.; Liu, H.; Zhang, X.; Li, X.; Zhang, G.; Cao, P. 3D Printed Micro-Electrochemical Energy Storage Devices: From Design to Integration. *Adv. Funct. Mater.* **2021**, *31*, No. 2104909.
(16) Sen, K.; Mehta, T.; Sansare, S.; Sharifi, L.; Ma, A. W. K.; Chaudhuri, B. Pharmaceutical Applications of Powder-Based Binder Jet 3D Printing Process − A Review. *Adv. Drug Delivery Rev.* **2021**, *177*, No. 113943.
(17) Miyanaji, H.; Momenzadeh, N.; Yang, L. Effect of Printing Speed on Quality of Printed Parts in Binder Jetting Process. *Addit. Manuf.* **2018**, *20*, 1−10.
(18) Parab, N. D.; Barnes, J. E.; Zhao, C.; Cunningham, R. W.; Fezzaa, K.; Rollett, A. D.; Sun, T. Real Time Observation of Binder Jetting Printing Process Using High-Speed X-Ray Imaging. *Sci. Rep.* **2019**, *9*, No. 2499.
(19) Moon, J.; Grau, J. E.; Knezevic, V.; Cima, M. J.; Sachs, E. M. Ink-Jet Printing of Binders for Ceramic Components. *J. Am. Ceram. Soc.* **2002**, *85*, 755−762.
(20) Young, T. An Essay on the Cohesion of Fluids. *Philos. Trans. R. Soc. London* **1805**, 65−87.
(21) Washburn, E. W. The Dynamics of Capillary Flow. *Phys. Rev.* **1921**, *17*, 273−283.
(22) Marmur, A. Penetration of a Small Drop into a Capillary. *J. Colloid Interface Sci.* **1988**, *122*, 209−219.
(23) Marmur, A. The Radial Capillary. *J. Colloid Interface Sci.* **1988**, *124*, 301−308.
(24) Denesuk, M.; Smith, G. L.; Zelinski, B. J. J.; Kreidl, N. J.; Uhlmann, D. R. Capillary Penetration of Liquid Droplets into Porous Materials. *J. Colloid Interface Sci.* **1993**, *158*, 114−120.
(25) Hapgood, K. P.; Litster, J. D.; Biggs, S. R.; Howes, T. Drop Penetration into Porous Powder Beds. *J. Colloid Interface Sci.* **2002**, *253*, 353−366.
(26) Chebbi, R. Absorption and Spreading of a Liquid Droplet Over a Thick Porous Substrate. *ACS Omega* **2021**, *6*, 4649−4655.
(27) Holman, R.; Cima, M.; Uhland, S.; Sachs, E. Spreading and Infiltration of Inkjet-Printed Polymer Solution Droplets on a Porous Substrate. *J. Colloid Interface Sci.* **2002**, *249*, 432−440.
(28) Miyanaji, H.; Momenzadeh, N.; Yang, L. Effect of Powder Characteristics on Parts Fabricated via Binder Jetting Process. *Rapid Prototyping J.* **2019**, *25*, 332−342.
(29) Bai, Y.; Wall, C.; Pham, H.; Esker, A.; Williams, C. B. Characterizing Binder−Powder Interaction in Binder Jetting Additive Manufacturing Via Sessile Drop Goniometry. *J. Manuf. Sci. Eng.* **2019**, *141*, No. 011005.
(30) Barui, S.; Ding, H.; Wang, Z.; Zhao, H.; Marathe, S.; Mirihanage, W.; Basu, B.; Derby, B. Probing Ink−Powder Interactions during 3D Binder Jet Printing Using Time-Resolved X-Ray Imaging. *ACS Appl. Mater. Interfaces* **2020**, *12*, 34254−34264.
(31) Ohnesorge, W. Die Bildung von Tropfen an Düsen Und Die Auflösung Flüssiger Strahlen. *J. Appl. Math. Mech.* **1936**, *16*, 355−358.
(32) Dini, F.; Ghaffari, S. A.; Jafar, J.; Hamidreza, R.; Marjan, S. A Review of Binder Jet Process Parameters; Powder, Binder, Printing and Sintering Condition. *Met. Powder Rep.* **2020**, *75*, 95−100.
(33) Mostafaei, A.; Elliott, A. M.; Barnes, J. E.; Li, F.; Tan, W.; Cramer, C. L.; Nandwana, P.; Chmielus, M. Binder Jet 3D Printing—Process Parameters, Materials, Properties, Modeling, and Challenges. *Prog. Mater. Sci.* **2021**, *119*, No. 100707.
(34) Boiziau, C.; Lecayon, G. Adhesion of Polymers to Metals: A Review of the Results Obtained Studying a Model System. *Surf. Interface Anal.* **1988**, *12*, 475−485.
(35) Lee, L.-H. Molecular Bonding and Adhesion at Polymer-Metal Interphases. *J. Adhes.* **1994**, *46*, 15−38.
(36) McCafferty, E. Acid-Base Properties of Surface Oxide Films. In *Surface Chemistry of Aqueous Corrosion Processes*; McCafferty, E., Ed.; SpringerBriefs in Materials; Springer International Publishing: Cham, 2015; Vol. *52*, pp 1−54.
(37) Yanez-Sanchez, S. I.; Lennox, M. D.; Therriault, D.; Favis, B. D.; Tavares, J. R. Model Approach for Binder Selection in Binder Jetting. *Ind. Eng. Chem. Res.* **2021**, *60*, 15162−15173.
(38) Bueche, F.; Coven, C. J.; Kinzig, B. J. Entanglement Effects in Concentrated Polymer Solutions from Viscosity Measurements. *J. Chem. Phys.* **1963**, *39*, 128−131.
(39) Fetters, L. J.; Lohse, D. J.; Richter, D.; Witten, T. A.; Zirkel, A. Connection between Polymer Molecular Weight, Density, Chain Dimensions, and Melt Viscoelastic Properties. *Macromolecules* **1994**, *27*, 4639−4647.
(40) El Aferni, A.; Guettari, M.; Kamli, M.; Tajouri, T.; Ponton, A. A Structural Study of a Polymer-Surfactant System in Dilute and Entangled Regime: Effect of High Concentrations of Surfactant and Polymer Molecular Weight. *J. Mol. Struct.* **2020**, *1199*, No. 127052.
(41) Graessley, W. W. The Entanglement Concept in Polymer Rheology. In. In *The Entanglement Concept in Polymer Rheology; Advances in Polymer Science;*; Advances in Polymer Science; Springer: Berlin, Heidelberg, 1974; Vol. *16*, pp 1−179.
(42) Shenoy, S. L.; Bates, W. D.; Frisch, H. L.; Wnek, G. E. Role of Chain Entanglements on Fiber Formation during Electrospinning of Polymer Solutions: Good Solvent, Non-Specific Polymer−Polymer Interaction Limit. *Polymer* **2005**, *46*, 3372−3384.
(43) Talbot, E. L.; Berson, A.; Brown, P. S.; Bain, C. D. Evaporation of Picoliter Droplets on Surfaces with a Range of Wettabilities and Thermal Conductivities. *Phys. Rev. E* **2012**, *85*, No. 061604.
(44) Munir, M. M.; Suryamas, A. B.; Iskandar, F.; Okuyama, K. Scaling Law on Particle-to-Fiber Formation during Electrospinning. *Polymer* **2009**, *50*, 4935−4943.
(45) Eda, G.; Shivkumar, S. Bead-to-Fiber Transition in Electrospun Polystyrene. *J. Appl. Polym. Sci.* **2007**, *106*, 475−487.
(46) Crane, N. B. Impact of Part Thickness and Drying Conditions on Saturation Limits in Binder Jet Additive Manufacturing. *Addit. Manuf.* **2020**, *33*, No. 101127.
(47) Williams, C. B.; Cochran, J. K.; Rosen, D. W. Additive Manufacturing of Metallic Cellular Materials via Three-Dimensional Printing. *Int. J. Adv. Manuf. Technol.* **2011**, *53*, 231−239.
(48) Lewis, R. Powder Binder Interactions in 3D Inkjet Printing. Masters thesis, Chalmers University of Technology: Gothenburg, Sweden, 2014.

https://doi.org/10.1021/acsomega.1c03857
ACS Omega 2022, 7, 5636−5645

(49) Zhao, H.; Ye, C.; Xiong, S.; Fan, Z.; Zhao, L. Fabricating an Effective Calcium Zirconate Layer over the Calcia Grains via Binder-Jet 3D-Printing for Improving the Properties of Calcia Ceramic Cores. *Addit. Manuf.* **2020**, *32*, No. 101025.
(50) Brunermer, D. T. Low Residual Carbon Binder for Binder Jetting Three-Dimensional Printing and Methods for Use of Same. U.S. Patent Application, US20200017699A12020.
(51) Alghunaim, A.; Kirdponpattara, S.; Newby, B. Z. Techniques for Determining Contact Angle and Wettability of Powders. *Powder Technol.* **2016**, *287*, 201−215.
(52) Kirdponpattara, S.; Phisalaphong, M.; Newby, B. Z. Applicability of Washburn Capillary Rise for Determining Contact Angles of Powders/Porous Materials. *J. Colloid Interface Sci.* **2013**, *397*, 169−176.
(53) Bruel, C.; Queffeulou, S.; Darlow, T.; Virgilio, N.; Tavares, J.R.; Patience, G.S. Experimental Methods in Chemical Engineering: Contact angle. *Can. J. Chem. Eng.* **2019**, *97*, 832−842.

https://doi.org/10.1021/acsomega.1c03857
ACS Omega 2022, 7, 5636−5645